JACS
JOURNAL OF THE AMERICAN CHEMICAL SOCIETY

Communication

pubs.acs.org/JACS

Temperature-Dependent Multidimensional Self-Assembly of Polyphenylene-Based "Rod–Coil" Graft Polymers

Yinjuan Huang,[†] Yiyong Mai,*[,†] Xiangwen Yang,[†] Uliana Beser,[‡] Junzhi Liu,[‡] Fan Zhang,[†] Deyue Yan,[†] Klaus Müllen,[‡] and Xinliang Feng*[,†,§]

[†]School of Chemistry and Chemical Engineering, Shanghai Jiao Tong University, 800 Dongchuan RD, Shanghai 200240, P. R. China
[‡]Max Planck Institute for Polymer Research, Ackermannweg 10, 55128 Mainz, Germany
[§]Department of Chemistry and Food Chemistry, Technische Universität Dresden, Mommsenstrasse 4, 01062 Dresden, Germany

Supporting Information

ABSTRACT: We present a novel type of "rod–coil" graft copolymer containing a polyphenylene backbone linked with poly(ethylene oxide) (PEO) side chains. Such graft copolymers manifest unprecedented temperature-dependent one-dimensional (1D) and two-dimensional (2D) self-assembly in solution. At 20 °C, which is higher than the crystallization temperature (T_c) of the PEO chains, the achiral graft copolymers self-organize into nanoribbons that twist into ∼30 μm ultralong helices with controlled pitch depending on the grafting ratio of the PEO chains. At 10 °C, which is lower than the T_c, quadrangular multilayer sheets of over 10 μm in lateral size are obtained. To our knowledge, this work presents the first example of controlled self-assembly of graft polymers into 1D helix and 2D sheet superstructures.

The supramolecular nanostructures of conjugated polymers with rigid backbones,[1] e.g., polyphenylene and polythiophene, have attracted considerable interest, owing to their unique electronic and optoelectronic properties.[1−7] In general, "rod–coil" conjugated polymers with both rigid conjugated and flexible polymer sequences can be synthons for self-assembly, the two primary types of which are rod–coil block copolymers and rod–coil graft copolymers. The self-assembly of rod–coil block copolymers has been extensively investigated in the past, and various ordered nanostructures, including spheres, cylinders, and vesicles, have been achieved.[2−7] For instance, Park and coworkers reported the self-assembly of a polythiophene-based rod–coil block copolymer, namely, poly[3-(2,5,8,11-tetraoxatridecanyl)-thiophene]-*block*-poly(ethylene glycol), resulting in ribbons and vesicles in tetrahydrofuran (THF)–water solutions depending on the water content.[7] In contrast, although the self-assembly of rod–coil graft copolymers, which comprise a rigid conjugated backbone with densely tethered polymeric side chains,[8] has been also studied in recent years,[9] it remains much less explored in many respects, including morphological control, hierarchical self-assembly, etc.

Herein, we demonstrate a novel type of rod–coil graft copolymer containing an expanded poly-*para*-phenylene backbone grafted with poly(ethylene oxide) (PEO) side chains (Figure 1). Featuring a unique rod–coil structure with a short average distance between neighboring PEO chains on the conjugated backbone, such graft copolymers exhibit remarkable temperature-dependent one-dimensional (1D) and two-dimensional (2D) hierarchical self-assembly behavior in solution above (20 °C) and below (10 °C) the T_c of the PEO chains, respectively. During the 1D self-assembly, the achiral graft copolymers organized into nanoribbons, which further bundled into ultralong helices with controlled pitch depending on the grafting ratio of the PEO chains (Figure 1A). The 2D self-assembly of the graft copolymers resulted in quadrangular multilayer sheets of micrometer-sized lateral dimensions (Figure 1B), for which an unprecedented self-assembly process from nanoribbons to "raft-like" nanostructures and, eventually, to the sheets was observed. To the best of our knowledge, such graft polymers represent the first example of polymers that can selectively self-assemble into 1D helix and 2D sheet superstructures.

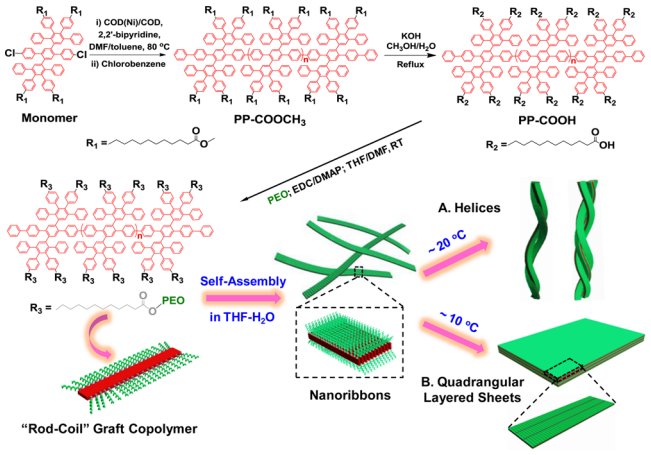

Figure 1. Schematic illustration of the synthesis of rod–coil graft copolymers containing a polyphenylene backbone grafted with PEO side chains as well as the temperature-dependent 1D and 2D hierarchical self-assembly process.

To prepare the rod–coil graft copolymers, laterally expanded poly-*para*-phenylene (i.e., poly-*para*-phenylene with dendritic tetraphenylbenzene substituents) decorated with $C_{10}H_{20}COOCH_3$ (PP-$COOCH_3$) was first synthesized by the

Received: July 17, 2015
Published: September 1, 2015

DOI: 10.1021/jacs.5b07487
J. Am. Chem. Soc. 2015, 137, 11602−11605

Yamamoto polymerization of a dichloro-substituted oligophenylene monomer (Figure 1 and Section 3 in the Supporting Information). After the hydrolysis of PP-$COOCH_3$ to PP-COOH, the graft copolymers were synthesized by the esterification of the carboxyl groups on PP-COOH with the hydroxyl groups at one end of 1K g/mol PEO (Figure 1). The successful grafting of the PEO chains onto the polyphenylene was validated by Fourier transform infrared spectroscopy (FTIR) (Figure S17) and nuclear magnetic resonance (NMR) analyses (Figure S18). Table 1 presents three graft copolymers with

Table 1. NMR and GPC Data for the Graft Copolymers

name	GP (%)[a]	$M_{n,\,calc}$[b]	$M_{n,\,GPC}$[c]	PDI[c]
PP-$COOCH_3$	N/A	N/A	21,400	1.13
GC-91	91	65,100	57,600	1.31
GC-55	55	47,800	42,100	1.27
GC-28	28	34,800	26,000	1.25

[a]PEO grafting percentages measured by NMR. [b]Calculated molecular weights based on M_n (GPC, PP-$COOCH_3$) and GPs. [c]M_n and polydispersity index (PDI) measured by GPC against a polystyrene standard; GPC curves are given in Figures S15 and S19.

different grafting percentages (GPs) of PEO chains, namely, GC-91, GC-55, and GC-28, with GPs of 91%, 55%, and 28%, respectively, as determined by NMR and supported by calculations based on elemental analyses (Pages S16–17). Gel permeation chromatography (GPC) results showed increased number-average molecular weights (M_n) compared with that of PP-$COOCH_3$ (Table 1). The M_n values measured by GPC ($M_{n,\,GPC}$) are slightly smaller than the calculated values ($M_{n,\,calc}$) based on the M_n of PP-$COOCH_3$ and the GPs. This difference is likely caused by the presence of carboxyl groups in the graft polymers, which enhance the adsorption of the polymers on GPC column and thus prolong their exclusion.[10]

The self-assembly of the rod–coil graft copolymers was performed through a cosolvent method[11] at different temperatures by considering the T_c of the tethered PEO chains (see below). Briefly, the copolymers were dissolved in THF, which is a common solvent for both polyphenylene and PEO, to produce a 10^{-3} mg mL^{-1} THF solution; under stirring, the solution was added dropwise (0.06 mL min^{-1}) to a 4-fold amount of pure water, a selective solvent for PEO. The mixed solution turned from colorless to light blue, suggesting the formation of polymer aggregates.

The self-assembly of GC-91 in the THF–water solution at 20 °C generated long helical nanostructures (Figure 2 and Figure S20). The transmission electron microscopy (TEM) samples prepared by freeze-drying gave the same helical structures as those in the vacuum-dried TEM samples, indicating the formation of helices in solution state.[12] Statistics based on 200 helices in the TEM images yielded an average diameter (D) of 44 ± 9 nm (Figure 2A) and lengths of 10–30 μm (up to ~30 μm, Figure S20A,B). Most of the helices comprised two or three ~15 nm wide 1D aggregates (Figure 2B,C); a minority of the helices (<10 number %) was multistranded (≥4 strands) (Figure S20D,E). High-resolution TEM (HRTEM) images revealed a ribbon-like structure of the 1D aggregates of ~15 nm width. For example, Figure 2D presents an HRTEM image of a double-stranded helix with a short untwisted section, in which the "width" of one strand is only ~4 nm, much smaller than that (~15 nm) of the other one. This exceptionally narrow width is attributed to the fact that a 4 nm thick ribbon is located vertically

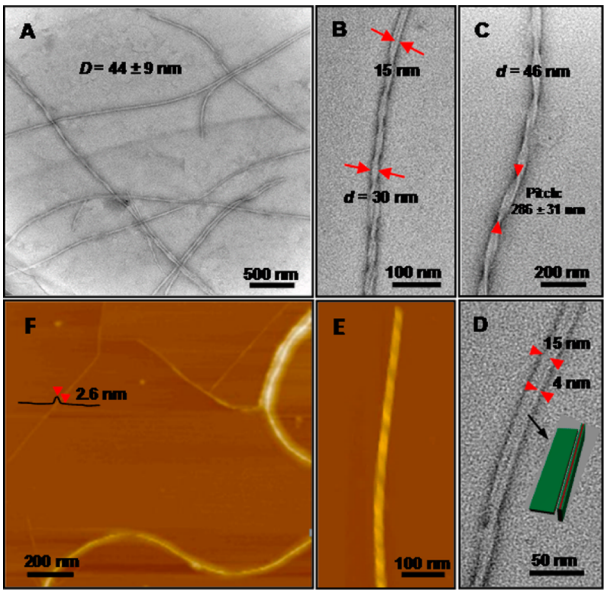

Figure 2. TEM and AFM images of the helices formed by the hierarchical self-assembly of the GC-91 graft copolymers in THF–water (v/v 1:4) at 20 °C. (A) A low-magnification TEM image of the helices (D denotes the average diameter); (B,C) high-magnification TEM images of the double- and triple-stranded helices with related sizes indicated (d expresses a diameter of a specific helix); (D) an HRTEM micrograph of an untwisted region in a double-stranded helix in which a ribbon-like aggregate is positioned vertical to the substrate (inset); (E) an AFM height profile of a helix; and (F) an AFM height image scanned after strong sonication of the helix dispersion in THF–water.

to the substrate under TEM investigation (inset of Figure 2D). As no chiral molecules were used in the self-assembly process, the coexistence of left- and right-handed helices observed by TEM is not surprising. Remarkably, the average diameter and pitch of the helices are tunable by varying the GP of the PEO chains. The statistics indicate that, as the GP of PEO decreases from 91% to 55% and 28%, the average diameter of the resultant helices decreases from 44 ± 9 nm to 39 ± 3 and 32 ± 2 nm, along with a decrease in the average pitch from 286 ± 31 nm to 208 ± 33 and 136 ± 20 nm, respectively (Figure S21).

The helical structure of the GC-91 aggregates was confirmed by atomic force microscopy (AFM) (Figure 2E). To further probe the composition of the helices, we attempted to disassemble the helices by strong sonication of their solutions. AFM profiles manifested that the helices consisted of ribbon-like aggregates with a width of ~15 nm and a thickness of ~2.6 nm (Figure 2F). These two values are very close to the calculated length (~15 nm) and width (~3.9 nm) of a graft copolymer molecule, respectively, suggesting that the ribbon-like aggregates are formed by the parallel alignment of the graft copolymers (see Section 4.3.1, Page S23).

In light of the above-mentioned results, in particular, the dimensions of the graft copolymer molecules and the resultant aggregates, we suggest a possible self-assembly mechanism, as illustrated in Figure 1. Driven by the hydrophobic interaction, the graft copolymers first self-assemble into ~15 nm wide and ~2.6 nm thick nanoribbons with a hydrophobic polyphenylene layer sandwiched by hydrophilic PEO coils. Owing to the relatively low PEO number density at both edges of the nanoribbons, they tend to associate to minimize the polyphenylene–water contact. However, the average distance between adjacent PEO chains in GC-91, GC-55, or GC-28 in the nanoribbons is estimated to be

DOI: 10.1021/jacs.5b07487
J. Am. Chem. Soc. 2015, 137, 11602–11605

~0.7, ~1.2, or ~2.2 nm, respectively (see Section 4.3.2, Pages S24–25). These distances are smaller than twice the radius of gyration (R_g = ~1.5 nm) of a 1K g/mol PEO chain at its end-free state in solution,[13] suggesting the existence of crowded PEO coils around the associated nanoribbons. Thus, the steric interaction among the PEO chains may cause a twist of the associated nanoribbons providing more peripheral space for the PEO coils and lead to the formation of 1D helical superstructures (Figure S22). The peripheral space around a helix within a small pitch can accommodate only a relatively small number of PEO chains; hence, with an increase in the PEO grafting ratio, the pitch of the helices increases accordingly.

Although supramolecular helix formation has been found in a few achiral linear polymers,[3,14] the current study presents the first example of helix formation by achiral graft polymers. More interestingly, we found that the graft copolymers self-organized into free-standing 2D quadrangular multilayer sheets at 10 °C. The sheet formation occurred over a period of days, with the aging of the as-prepared solution of the GC-91 aggregates at 10 °C. Within 5 h of aging, TEM images (Figure 3A) revealed a large number of raft-like assemblies (called "rafts") that consisted of ~15 nm wide 1D nanostructures (inset of Figure 3A); the width was similar to that of the above-discussed nanoribbons. Moreover, the thickness of the rafts was ~2.6 nm (Figure 3B), the same as that of the nanoribbons. Therefore, it is reasonable to believe that the rafts are single-layered and formed by the planar alignment of the nanoribbons. Remarkably, with the aging of the solution, the rafts grew to narrow nanosheets (Figure 3C,D) and eventually to quadrangular sheets after ca. 10 days (Figure 3E–H). The thickness of the quadrangular sheets was greater than that of the rafts, suggesting a multilayer feature of the sheets. The quadrangular sheets suspended in solution were also observed by optical microscopy (Figure S23), confirming that the sheets were formed in solution. Moreover, dynamic light scattering (DLS) analyses revealed an obvious increase in the hydrodynamic diameter of the GC-91 assemblies with the aging of the solution at 10 °C, whereas no big change was found in the hydrodynamic size of the GC-91 helices in solution at 20 °C (Figure S24). The results confirm the gradual growth of the GC-91 assemblies in solution at 10 °C.

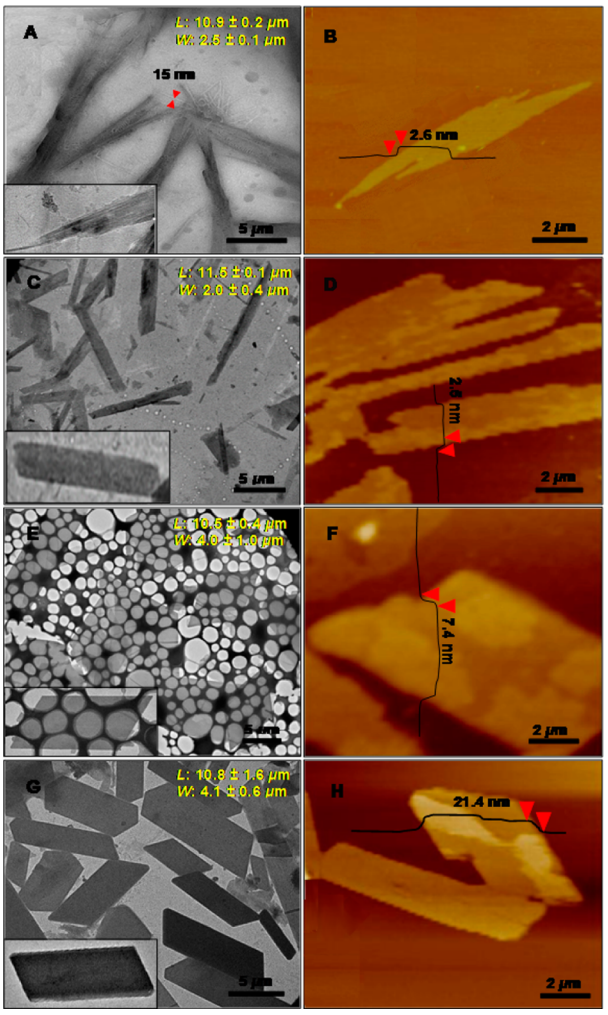

Figure 3. TEM and AFM images of the 2D aggregates formed by the hierarchical self-assembly of GC-91 in THF–water (v/v 1:4) at 10 °C after (A,B) 5 h, (C,D) 1 day, (E,F) 5 days, and (G,H) 10 days. The average lengths (L), widths (W), and thicknesses of the aggregates are indicated in the corresponding TEM and AFM images.

It is known that PEO crystallization in organic media may contribute to the solution growth of multilayer rhombus crystals of some PEO-containing block copolymers, e.g., PEO-*b*-polycaprolactone in hexanol.[15,16] In the present study, differential scanning calorimetry (DSC) analyses of GC-91 revealed a T_c of ~16 °C for the grafted 1K g/mol PEO chains (Figure S25A). Micro-DSC measurements gave a T_c of ~13 °C for the PEO chains in the GC-91 aggregates in THF–water (Figure S25B). Apparently, the 1D and 2D self-assembly of GC-91 occurred above and below the T_c of the PEO chains, respectively. After GC-91 self-organized into nanoribbons (Figure 1), a short average distance of ~0.7 nm between neighboring PEO chains on the polyphenylene backbone resulted in a high number density of PEO chains at the ribbon surface, which exceeded the onset density for the crystallization of the chains below their T_c (see calculations in Section 4.3.2, Pages S24–25).[16,17] Thus, the crystallization and the resulting compact state of the PEO chains may favor the transformation of the nanoribbons into sheet-like structures.[18] In contrast, the PEO chains at the surfaces of the nanoribbons formed by GC-55 or GC-28 cannot crystallize due to the low density of the chains (Section 4.3.2, Pages S24–25),[16,17] which accounts for the formation of only helices rather than sheets under similar experimental conditions. As the onset density of PEO crystallization is determined by both the dimension of PEO and the average distance between neighboring PEO chains on the polyphenylene, the length of PEO chains, in addition to the GP, can also affect the 2D self-assembly of the graft copolymers. For instance, owning a GP of ~90%, the graft copolymer with 500 g/mol PEO side chains did not form quadrangular multilayer sheets under similar conditions, due to the reduced length of the PEO coils.

To further investigate how the multilayer sheets are related to the crystallization of the PEO chains, the THF–water solution of the sheets was dialyzed against water to remove THF at 10 °C. Interestingly, we found that the multilayer sheets developed into rafts after the removal of the THF (Figure S26A,B). Increasing the temperature of the THF–water solution from 10 to 25 °C also yielded rafts. Such disorganization, the reverse step of the sheet formation, may be caused by the expansion of the PEO coils in solution from a compact crystalline state in the presence of organic media (THF in this case) or below their T_c.[16,18] Moreover, an attempt was made to elucidate the crystal structure of the sheets by electron diffraction (ED). However, no diffraction patterns were observed (Figure S26C), probably

DOI: 10.1021/jacs.5b07487
J. Am. Chem. Soc. 2015, 137, 11602–11605

due to the destruction of the crystal structure at temperatures higher than the T_c of the 1K g/mol PEO upon the irradiation of electron beams.[19]

The optical properties of the GC-91 assemblies in THF–water solutions were studied by ultraviolet–visible (UV–vis) and photoluminescence (PL) spectroscopies (Figure 4). The

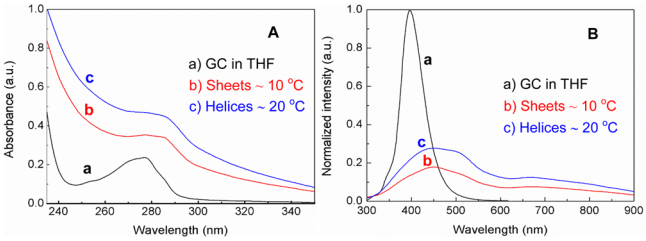

Figure 4. (A) UV–vis and (B) photoluminescence spectra of GC-91 in THF as well as of the helices and the sheets in THF–water (v/v 1:4) at different temperatures (concentration: 2×10^{-4} mg mL^{-1}).

maximum absorption of the helices and the sheets were red-shifted to ~290 nm, compared with 280 nm of GC-91 in THF (Figure 4A), indicative of intermolecular π–π interactions associated with the aggregation of GC-91.[3] The PL spectra revealed a distinct quenching of the photoluminescence of both the helices and the sheets in THF–water (Figure 4B). The PL spectra of the helices remained almost unchanged with the aging of their solution at 20 °C over 10 days, suggesting their good stability in solution;[3] however, the PL spectra of the assemblies obtained at 10 °C showed a consecutive quenching of the photoluminescence (Figure S27), most probably due to the progressive formation of the sheets.

In summary, we prepared a novel type of rod–coil graft copolymer containing a poly-*para*-phenylene backbone grafted with 1K g/mol PEO chains. Remarkably, these polymers performed temperature-dependent 1D and 2D self-assembly in solution. At 20 °C, which is above the T_c of the PEO chains, the achiral graft copolymers self-organized into 1D nanoribbons that further bundled into ~30 μm helices. At 10 °C, which is below the T_c, the self-assembly of the graft copolymers, driven by the crystallization of the tethered PEO chains, resulted in progressive growth of nanoribbons into rafts and eventually into quadrangular multilayer sheets with lateral dimensions of over 10 μm. These novel rod–coil graft polymers provide new opportunities for the controlled preparation of 1D helix and 2D superstructures as well as offer a new system for the fundamental studies on the self-assembly of conjugated polymers, including morphological control, thermodynamics and kinetics, potential applications, etc.

■ ASSOCIATED CONTENT

Supporting Information

The Supporting Information is available free of charge on the ACS Publications website at DOI: 10.1021/jacs.5b07487.

Experiments, supporting figures, and calculations (PDF)

■ AUTHOR INFORMATION

Corresponding Authors

*mai@sjtu.edu.cn

*xinliang.feng@tu-dresden.de

Notes

The authors declare no competing financial interest.

■ ACKNOWLEDGMENTS

The authors thank the financial support from the 973 Programs of China (2012CB933404 and 2013CBA01602), the Natural Science Foundation of China (21320102006 and 21304057), the Natural Science Foundation of Shanghai (13ZR1421200), the Program for Eastern Scholar in Shanghai, and the MPI Partner Group Project for Polymer Chemistry of Graphene Nanoribbons. We also thank the Instrumental Analysis Center of Shanghai Jiao Tong University for some measurements.

■ REFERENCES

(1) (a) Li, C.; Liu, M.; Pschirer, N. G.; Baumgarten, M.; Müllen, K. *Chem. Rev.* **2010**, *110*, 6817. (b) Bonillo, B.; Swager, T. M. *J. Am. Chem. Soc.* **2012**, *134*, 18916. (c) Liu, J.; Li, B.; Tan, Y.; Giannakopoulos, A.; Sanchez-Sanchez, C.; Beljonne, D.; Ruffieux, P.; Fasel, R.; Feng, X.; Müllen, K. *J. Am. Chem. Soc.* **2015**, *137*, 6097.

(2) Jenekhe, S. A.; Chen, X. L. *Science* **1998**, *279*, 1903.

(3) Lee, E.; Hammer, B.; Kim, J.-K.; Page, Z.; Emrick, T.; Hayward, R. C. *J. Am. Chem. Soc.* **2011**, *133*, 10390.

(4) Patra, S. K.; Ahmed, R.; Whittell, G. R.; Lunn, D. J.; Dunphy, E. L.; Winnik, M. A.; Manners, I. *J. Am. Chem. Soc.* **2011**, *133*, 8842.

(5) Zheng, Y.; Zhou, H.; Liu, D.; Floudas, G.; Wagner, M.; Koynov, K.; Mezger, M.; Butt, H.-J.; Ikeda, T. *Angew. Chem., Int. Ed.* **2013**, *52*, 4845.

(6) Liu, N.; Qi, C. G.; Wang, Y.; Liu, D. F.; Yin, J.; Zhu, Y. Y.; Wu, Z. Q. *Macromolecules* **2013**, *46*, 7753.

(7) Kamps, A. C.; Cativo, M. H. M.; Fryd, M.; Park, S.-J. *Macromolecules* **2014**, *47*, 161.

(8) (a) Sheiko, S. S.; Sumerlin, B. S.; Matyjaszewski, K. *Prog. Polym. Sci.* **2008**, *33*, 759. (b) Rzayev, J. *ACS Macro Lett.* **2012**, *1*, 1146.

(9) (a) Yao, J. H.; Mya, K. Y.; Shen, L.; He, B.; Li, L.; Li, Z.; Chen, Z.; Li, X.; Loh, K. P. *Macromolecules* **2008**, *41*, 1438. (b) Lin, J.; Zhu, G.; Zhu, X.; Lin, S.; Nose, T.; Ding, W. *Polymer* **2008**, *49*, 1132. (c) Cai, C.; Lin, J.; Chen, T.; Tian, X. *Langmuir* **2010**, *26*, 2791. (d) Miyake, G. M.; Weitekamp, R. A.; Piunova, V. A.; Grubbs, R. H. *J. Am. Chem. Soc.* **2012**, *134*, 14249.

(10) Turner, S. R.; Walter, F.; Voit, B. I.; Mourey, T. H. *Macromolecules* **1994**, *27*, 1611.

(11) Mai, Y.; Eisenberg, A. *Chem. Soc. Rev.* **2012**, *41*, 5969.

(12) Azzam, T.; Eisenberg, A. *Langmuir* **2010**, *26*, 10513.

(13) The R_g for a PEO chain at its end-free state in solution is estimated using $R_g^2 = b^2N_b/6$ from Rubenstein, M.; Colby, R. H. *Polymer Physics*; Oxford University Press: New York, 2004, where b = 0.8 nm for PEO.

(14) (a) Zhong, S.; Cui, H.; Chen, Z.; Wooley, K. L.; Pochan, D. J. *Soft Matter* **2008**, *4*, 90. (b) Dupont, J.; Liu, G.; Niihara, K.-I.; Kimoto, R.; Jinnai, H. *Angew. Chem., Int. Ed.* **2009**, *48*, 6144.

(15) Sun, J. R.; Chen, X. S.; He, C. L.; Jing, X. B. *Macromolecules* **2006**, *39*, 3717.

(16) Van Horn, R. M.; Zheng, J. X.; Sun, H.-J.; Hsiao, M.-S.; Zhang, W.-B.; Dong, X.-H.; Xu, J.; Thomas, E. L.; Lotz, B.; Cheng, S. Z. D. *Macromolecules* **2010**, *43*, 6113.

(17) Zheng, J. X.; Xiong, H.; Chen, W. Y.; Lee, K.; Van Horn, R. M.; Quirk, R. P.; Lotz, B.; Thomas, E. L.; Shi, A.-C.; Cheng, S. Z. D. *Macromolecules* **2006**, *39*, 641.

(18) Rizis, G.; van de Ven, T. G. M.; Eisenberg, A. *Angew. Chem., Int. Ed.* **2014**, *53*, 9000.

(19) Egerton, R. F.; Malac, P.; Li, M. *Micron* **2004**, *35*, 399.

DOI: 10.1021/jacs.5b07487
J. Am. Chem. Soc. 2015, 137, 11602–11605